RHEOLOGICAL SOLUTIONS, INC.

8101 Cessna Avenue
Gaithersburg, MD 20879
(301) 963-7157
(301) 990-3155 FAX

VIBRATION CONTROL USING CHAOTIC MOTION STABILIZERS

A Final Report for the
Ballistic Missile Defense Organization (BMDO) and the U.S. Army Space and Strategic Defense Command (USASSDC)

Prepared by

David L. Don
Prinicpal Investigator
Rheological Solutions, Inc.
Gaithersburg, MD

Edward S. Regan
Senior Engineer
Rheological Solutions, Inc.
Gaithersburg, MD

Contract Number
DASG60-94-C-0059

Reporting Period
6 months

Contract Period
5 JUNE 1994 - 5 DECEMBER 1994

Date
20 DECEMBER 1994

SECURITY CLASSIFICATION OF THIS PAGE

REPORT DOCUMENTATION PAGE

Form Approved OMB No. 0704-0188

1a. REPORT SECURITY CLASSIFICATION: Unclassified	1b. RESTRICTIVE MARKINGS: N/A
2a. SECURITY CLASSIFICATION AUTHORITY: N/A	3. DISTRIBUTION/AVAILABILITY OF REPORT: Unlimited
2b. DECLASSIFICATION/DOWNGRADING SCHEDULE: N/A	
4. PERFORMING ORGANIZATION REPORT NUMBER(S):	5. MONITORING ORGANIZATION REPORT NUMBER(S):
6a. NAME OF PERFORMING ORGANIZATION: Rheological Solutions, Inc 6b. OFFICE SYMBOL (If applicable):	7a. NAME OF MONITORING ORGANIZATION: U.S. Army Space and Strategic Defense Command (USASSDC)
6c. ADDRESS (City, State, and ZIP Code): 8101 Cessna Avenue Gaithersburg, MD 20879	7b. ADDRESS (City, State, and ZIP Code): PO Box 1500 CSSD-CM-TK Huntsville, AL 35807-3801
8a. NAME OF FUNDING/SPONSORING ORGANIZATION: BMDO 8b. OFFICE SYMBOL (If applicable):	9. PROCUREMENT INSTRUMENT IDENTIFICATION NUMBER: DASG60-94-C-0059
8c. ADDRESS (City, State, and ZIP Code): Director, BMDO 7100 Defense Washington DC 20301-7100	10. SOURCE OF FUNDING NUMBERS PROGRAM ELEMENT NO. / PROJECT NO. / TASK NO. / WORK UNIT ACCESSION NO.

11. TITLE (Include Security Classification): Vibration Control Using Chaotic Motion Stabilizers

12. PERSONAL AUTHOR(S): David L. Don and Edward S. Regan

13a. TYPE OF REPORT	13b. TIME COVERED	14. DATE OF REPORT (Year, Month, Day)	15. PAGE COUNT
Final	FROM 6/94 TO 12/94	94/12/20	28

16. SUPPLEMENTARY NOTATION

17. COSATI CODES			18. SUBJECT TERMS (Continue on reverse if necessary and identify by block number)
FIELD	GROUP	SUB-GROUP	Vibrations, Chaos, Smart, Noise, Damping Active Control, Electrorheological, Stabilizer

19. ABSTRACT (Continue on reverse if necessary and identify by block number)

Chaotic Motion Stabilizers transform chaotic behavior into predictable periodic motion. Our product enhances the performance of active damping systems, eliminates the need for damping devices in some applications, and increases the variability of passive damping methods. We have based our product on the observance that chaotic attractors typically have infinite numbers of unstable periodic orbits. The device attempts to stabilize existing orbits in the attractor -- not create new ones. The process is straight forward. First, determine unstable periodic orbits embedded in the chaotic attractor. Examine these orbits and choose ones that yield improved system performance. Finally, tailor small-time dependent parameter perturbations to stabilize the orbit. To make the necessary system parameter changes that transform chaotic motion into periodic motion, we will utilize electrorheological (ER) materials. For Phase I research we modeled the behavior of an ER magnetoelastic system and incorporated our control algorithm into the model. We then compared the theoretical results with experimental testing where similarities were observed.

20. DISTRIBUTION/AVAILABILITY OF ABSTRACT	21. ABSTRACT SECURITY CLASSIFICATION
☒ UNCLASSIFIED/UNLIMITED ☐ SAME AS RPT. ☐ DTIC USERS	Unclassified
22a. NAME OF RESPONSIBLE INDIVIDUAL: C. McCollough	22b. TELEPHONE (Include Area Code): (205) 955-4825 / 22c. OFFICE SYMBOL

DD Form 1473, JUN 86 — Previous editions are obsolete. — SECURITY CLASSIFICATION OF THIS PAGE

TABLE OF CONTENTS

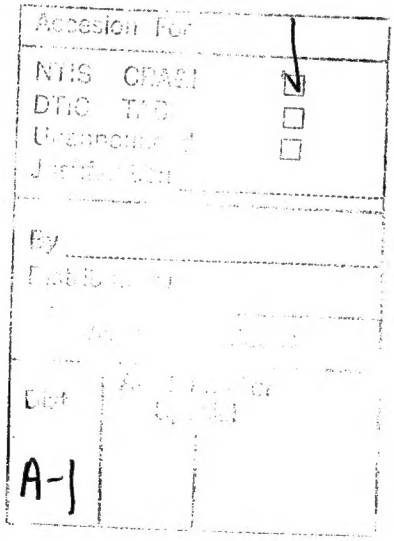

I. INTRODUCTION

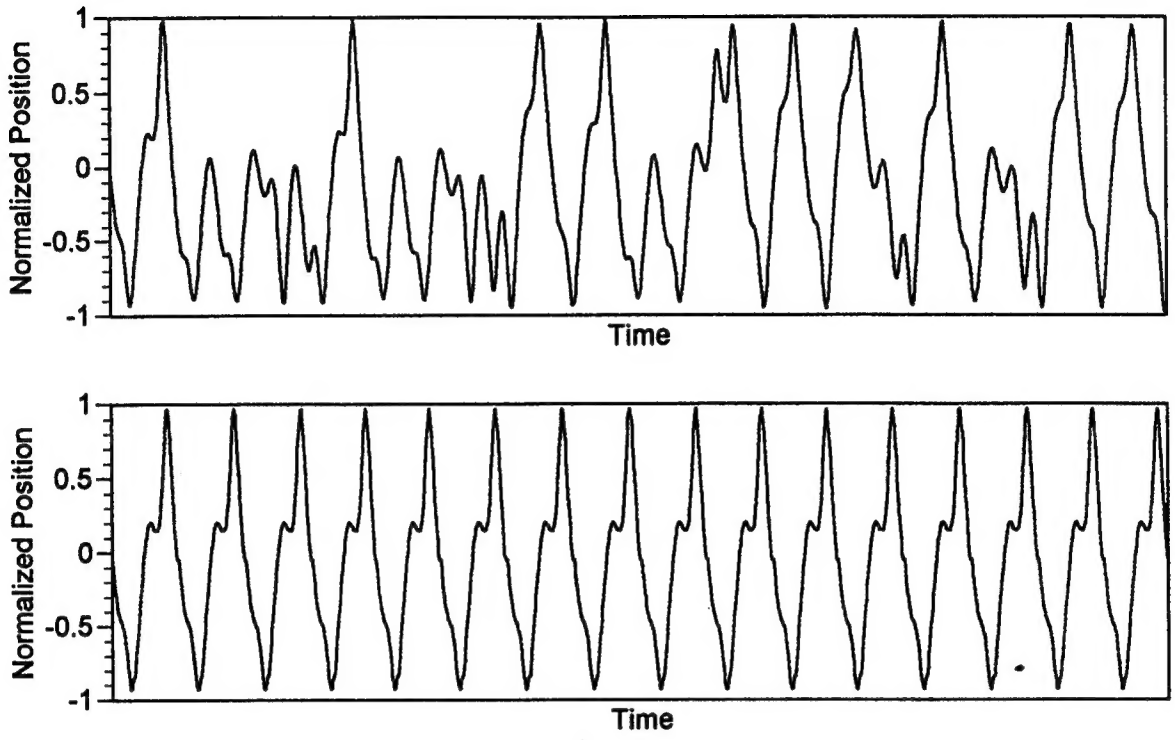

Figure 1. Controlling the Behavior of a Chaotic System

The objective of a ballistic missile defense (BMD) sensor system is to find enemy targets, aim weapons, and determine whether the weapon destroyed the selected target. This objective is broken into three respective functions: discrimination, pointing and tracking, and kill assessment. Sensitive optical and electronic equipment aboard interceptors and satellites demand aiming accuracies on the order of a tenth of a micro radian. Vibrations caused by thermo-mechanical flutter, thruster firing, and/or structure borne noise significantly reduce sensor precision. Suppression systems are therefore vital for the development of highly accurate BMD weapon systems.

Our intention is to develop an innovative control vibration device called a Chaotic Motion Stabilizer for BMD applications. Chaotic Motion Stabilizers transform chaotic behavior into predictable periodic motion as Figure 1 illustrates. Our product enhances the performance of active damping systems, eliminates the need for damping devices in some applications, and increases the variability of passive damping methods.

Chaotic Motion Stabilizers could make active damping systems a more attractive alternative in some applications, and improve the effectiveness and simplify the control algorithm in others. Active damping uses anti-noise to cancel extraneous vibrations. This entails adding anti-noise or noise 180 degrees out of phase with the unwanted vibrations to mirror the incoming noise. When the two add together, the result is silence. There are

two active approaches -- feedfoward and feedback control systems. In both of these systems, the effectiveness of the technique hinges on the systems' ability to **predict** the incoming noise at the location where anti-noise is applied.

In a feedback scheme, a down stream microphone returns a sampled signal to the controller. The controller then sends an anti-noise signal to the speaker that neutralizes the incoming vibration. A feedback system will only work for predictable periodic motions. The fundamental feedback problem is the inability to predict the chaotic behavior of an upstream location. Figure 2 clearly illustrates this problem. A paper stream with randomly colored black and white dots is moving at a constant rate across a plane. If we know the color of the dot at location 1, it tells us nothing about the color of the dot at location 0, upstream, because the system is random. The only way to know the behavior of an upstream location is when the dots are periodically placed. In the same manner, active feedback can only work in situations where noise is periodic or predictable. When faced with chaotic motions, a feedfoward system is more appropriate.

In feedfoward active control an upstream microphone samples the magnitude and phase of the incoming noise. A controller uses the sample to drive a downstream speaker that provides the anti-noise. A feedforward systems effectiveness is dependent on the ability to predict the magnitude and phase of the noise at the downstream speaker location. The method works for both chaotic and periodic motions assuming two favorable circumstances. First, they can create a time delay from the sampled noise to the speaker and the time delay is slow enough for the control electronics to act. Second, the sampled motion upstream does not change before it reaches the anti-noise speaker. Figure 3 more clearly illustrates feedforward control. The same paper stream in Figure 2 is moving at a constant rate of 1 cm/sec across a plane. If we know the dot is black at location 1, in 1 second the dot will still be black at location 2, 1cm downstream. We can use the same analysis for feedforward active control. Feedforward systems have shown success in neutralizing chaotic noise in air ducts and mufflers.

Feedback and feedforward active systems are not effective in many applications. Active feedback systems are not capable of neutralizing chaotic noises that appear in most vibration applications. They can only cancel periodic signals. Feedforward systems can neutralize chaotic motions, but the necessary delay times required for effective performance are too short in structural applications. The wave speeds in solids are faster than the electronic algorithms needed for digital analysis -- the unwanted vibrations pass the antinoise actuator before it has a chance to analyze the upstream sensor sample. In addition, many structural applications cannot use one-dimensional noise source approximations as feedforward systems depend upon. At a single location on a structure the source of noise is three dimensional and could come from a combination of the infinite number of directional vectors surrounding that location. The inherent nature of chaotic control is not dependent on a noise source, in fact, it relies on the complexities of the incoming noise. With their ability to transform chaotic behavior to predictable periodic motion, Chaotic Motion Stabilizers make active feedback possible eliminating the need for feedforward systems altogether.

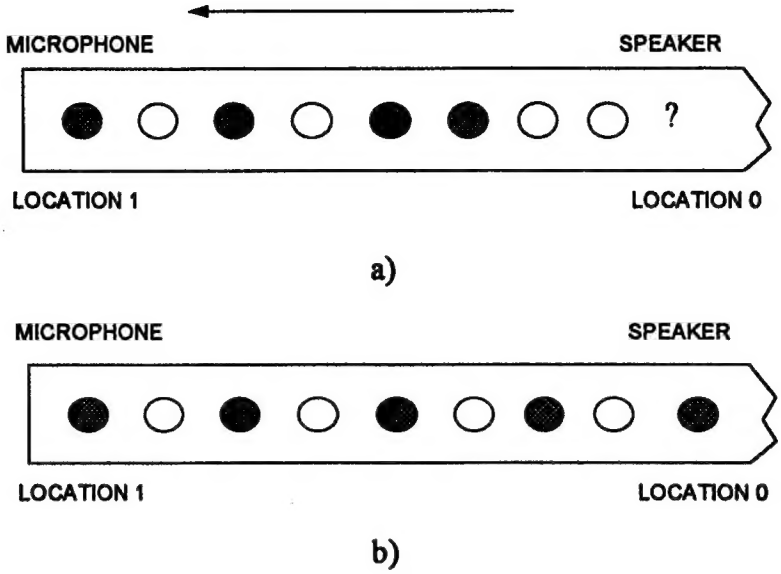

Figure 2. Feedback Phenomenon of a)Random Dots b)Periodic Dots

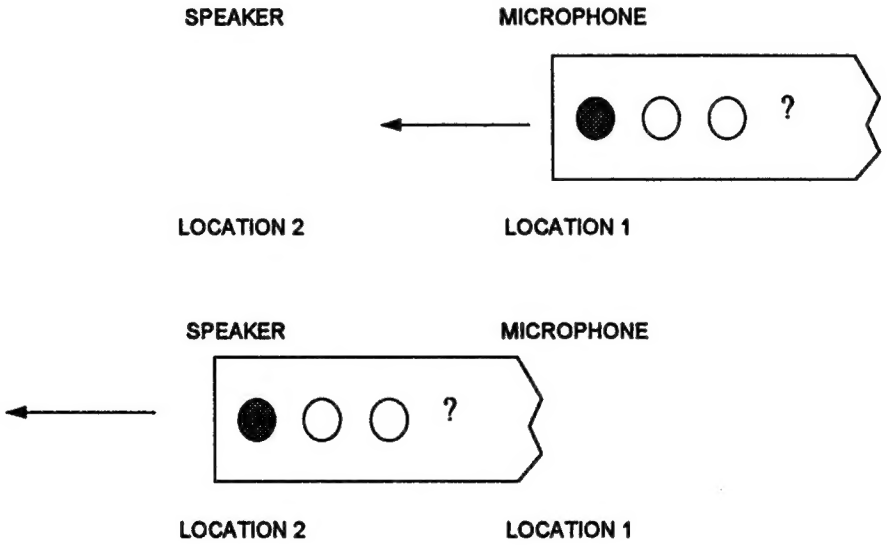

Figure 3. Feedforward Control

Chaotic Motion Stabilizers could also replace damping systems in some electronics and instrumentation. Employing a stabilizer could eliminate the need for such devices since on board electronic instrumentation could compensate for the predictable motions. End users would prefer semi-active electronic compensation versus active cancellation because of an active system's adverse collateral effects. These include introducing vibrations into other areas of the system and increasing the vibration to catastrophic levels if the system fails. If a Chaotic Motion Stabilizer fails, it is acts as a passive damper.

They also offer an innovative approach to passive damping approaches because of their variability. The passive damping approach requires the application of vibration absorbing materials either housed in a damper or directly applied to, the desired system. Vibration absorbent materials include fiberglass, acoustic foams, rubber, polymer blends, and fluids. When strained these materials absorb the mechanical energy and transform it into heat; thereby reducing some of the vibrational response. The limitation of the method rests with the damping material's mechanical behavior. Their damping properties are dependent on temperature and frequency where optimal damping occurs at single location. With a Chaotic Motion Stabilizer, one can select infinite numbers of periodic orbits that could improve system performance in a diverse range of environments.

Table 1 summarizes the strengths and weaknesses of the different approaches to vibrational damping.

PRODUCT	STRENGTHS	WEAKNESSES
Chaotic Motion Stabilizers	Enhances the performance of active systems Variable damping through selection of infinite numbers of periodic orbits Uses a semi-active approach that won't cause catastrophic failure	Unproven technology Costly
Passive Damping Devices	Low Cost Simple to apply	Limited range of operational effectiveness Ineffective for many applications
Active Damping Systems	Eliminates unwanted predictable vibrations completely	Cannot neutralize chaotic motions in many applications Costly

Table 1. Competitive Matrix of Damping Systems

II. METHODOLOGY

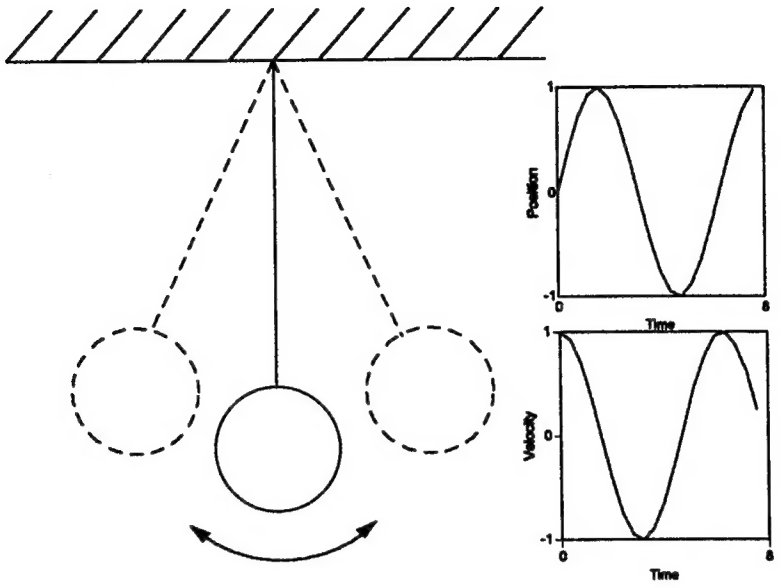

Figure 4. Dynamic Behavior of an Undamped Swinging Pendulum

In the past, scientists believed they could predict the future indefinitely by knowing the laws of nature and the initial conditions of the system. For example, with a knowledge of the laws of gravity, Newton's laws, and the planets initial conditions -- position, mass, and velocity; astronomers can predict planetary motions thousand of years into the future. The inability to predict the future in other systems such as the weather and turbulence was blamed on a lack of knowledge of the laws governing the system, the complexity of the system, and/or the inability to measure initial conditions. They assumed that if we obtained all of this information, one could predict the behavior of seemingly random systems much like planetary motion.

Chaos theory killed this idea. Simple deterministic systems with only a few elements generate seemingly random behavior. We now accept that unpredictability as fundamental to chaotic systems. The reason -- a chaotic systems' sensitivity to initial conditions. Two identical systems with very small differences in initial conditions diverge exponentially. Minute differences become so amplified that although the system is predictable in the short term, its long-term behavior is completely unpredictable.

State-space representations are useful tools for observing and explaining chaotic systems. It is an abstract space whose coordinates are governed by the number of initial conditions needed to solve the differential equations modeling the system. The swinging pendulum illustrates a simple example of state-space. It has two state variables: angular position and velocity. In the undamped case, Figure 4, the pendulum swings back and forth for all

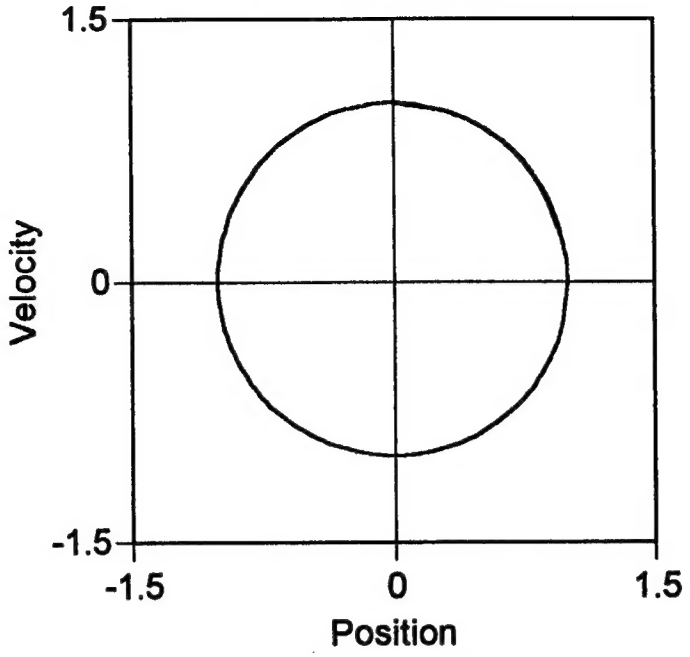

Figure 5. State-space Representation of a Swinging Pendulum

of time. The position and velocity states with respect to time are shown. A state-space representation combines the two as Figure 5 illustrates. The steady-state response represents a linear attractor whose trajectories are bound within a region of space, in this case a circle. The state-space representation of a chaotic attractor is shown in Figure 6. The axes represent states of the system and the loops represent the dynamic trajectory of the states with respect to time. The paths never retrace, but are bound within regions of state-space known as chaotic attractors. These attractors depict collections of many orderly behaviors, none of which exclusively dominates.

We have based our product on the observance that chaotic attractors typically have infinite numbers of unstable periodic orbits. The device attempts to stabilize existing orbits in the attractor -- not create new ones. The process is straight forward. First, determine unstable periodic orbits embedded in the chaotic attractor. Examine these orbits and choose ones that yield improved system performance. Finally, tailor small-time dependent parameter perturbations to stabilize the orbit.

To make the necessary system parameter changes that transform chaotic motion into periodic motion, we will utilize electrorheological (ER) materials. These materials are suspensions of dielectric particles in non-polar liquids that exhibit dramatic reversible changes in rheological response when exposed to an electric field. A simplified physical description of the behavior is that the material transforms from a liquid to a solid-like gel when exposed to electric fields. The mechanism for this transformation is the formation of particle chains across the field as displayed in Figure 7[1-5]. When formed, the chains restrict the flow of the liquid matrix.

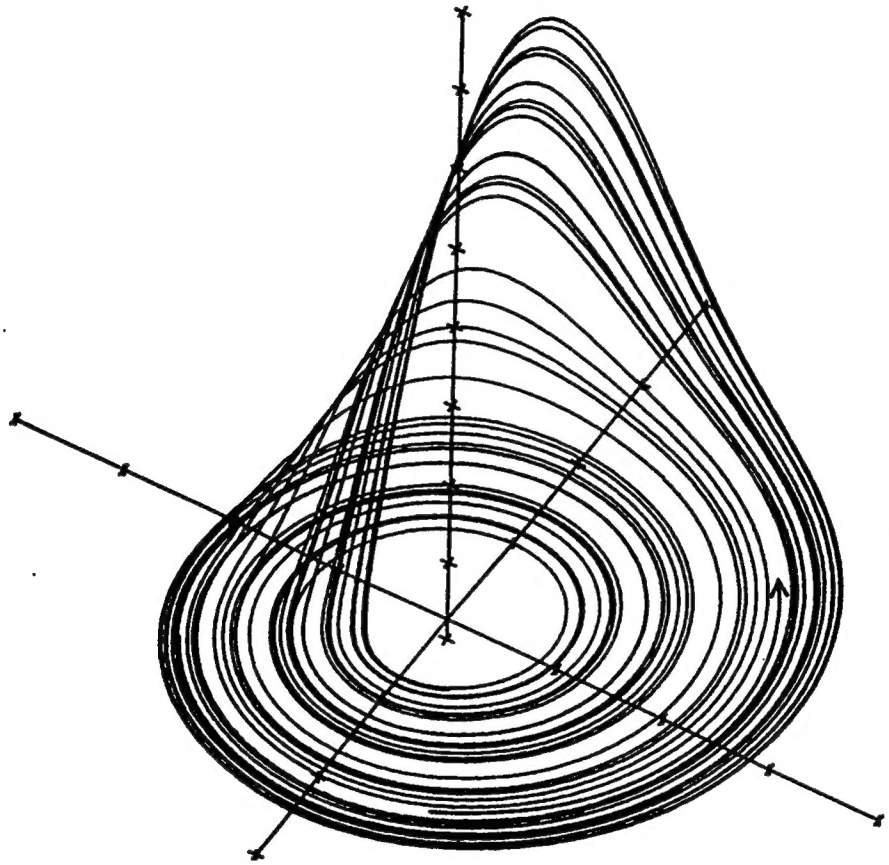

Figure 6. The Rossler Attractor [22]

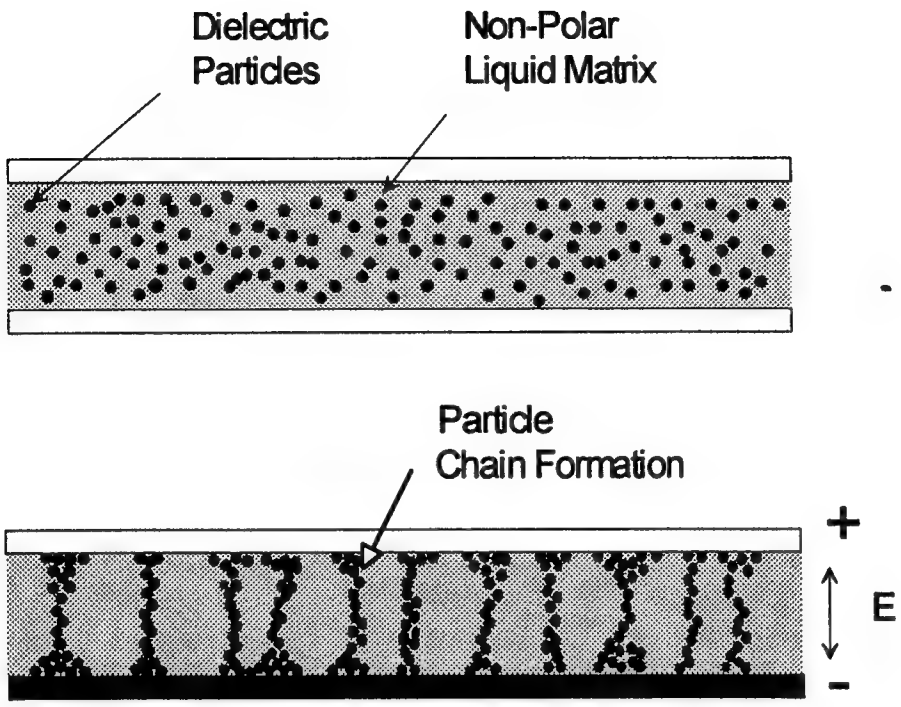

Figure 7. ER Phenomenon a)no electric field b)with electric field applied

Ott et al. [6,7] first demonstrated that one can convert chaotic motion to periodic motion. They accomplished this by controlling the system about one of the many unstable periodic orbits embedded in the chaotic attractor through small time-dependent perturbations of an accessible system parameter. The method, known as the OGY algorithm, is different from other published methods that typically make large changes in system behavior and attempt to eliminate chaos all together. In many cases the latter requires changes in the system that are too expensive or impossible.

Several studies have investigated their techniques. Hunt [8] eliminated the need for a Poincare section by using direct system measurement. This made the method converge much faster enabling the manipulation of rapidly changing systems. Shinbrot et al. [9] devised a method for forcing the system into the orbit of choice much faster from any arbitrary initial condition. Dressler and Nitsche [10] were able to improve overall system performance by taking into account past parameter changes. Ditto et al. [11,12] achieved the first experimental control of chaos by controlling a buckling magnetoelastic beam. Hall et al. [13] investigated chaotic control of a simple buckled beam. They stabilized the motion by moving the system out of the chaotic parameter region. Rollins et al. [14] discussed a recursive proportional feedback algorithm for highly dissipative systems using an adaptation from Dressler and Nitsche [15]. Garfinkel et al. [16] successfully controlled, where previous methods failed, heart arrhythmia in animals using an OGY pacemaker. The system we have controlled was first examined by Moon and Holmes

[17]. They developed a computer simulation of the magnetoelastic attractor and compared those results with experimental testing. Their results showed qualitative similarities.

Rheological Solutions has divided the product line into discrete and distributed devices. Discrete devices absorb energy at a point source. Dashpots, shock absorbers, and engine mounts are types of discrete devices. They are useful when the source of noise is isolated. The idea is to stabilize the vibration before the energy reaches its target. Distributed devices are used when we need to change the behavior of an entire structure. Distributed damping methods include constrained layer damping and damping coatings. These systems absorb energy from the structure as a whole and are ideal for attenuating low amplitude noise at multiple locations and high frequencies. Their application is limited by their inability to absorb large strain amplitudes and are generally less efficient than discrete devices. For this investigation, we studied the control of a distributed Chaotic Motion Stabilizer.

III. RESULTS

The basic recipe for chaotic control contains three steps. First, identify periodic orbits embedded within the attractor. Second, determine the local dynamics of those orbits. Finally, stabilize an orbit around a fixed point coordinate.

IDENTIFY EMBEDDED PERIODIC ORBITS

As previously discussed, the analysis of chaotic systems are best illustrated using a state-space representation . The state variables appear as first-order equations,

$$\frac{d\overline{X}}{dt} = F(\overline{X}, p) \tag{1}$$

where p is the control parameter. $\overline{X}$ is a set of physical quantities that completely specifies the state of the system,

$$\overline{X} = \left(x_0(t), x_1(t), x_2(t), \ldots, x_{m-1}(t)\right) \tag{2}$$

and m is the number of state variables. One can observe many unstable periodic orbits embedded within chaotic attractors. We define an orbit as a series of points $\xi_1, \xi_2, \xi_3, \ldots$ such that,

$$\xi_n = \left(x_0(t_n), x_1(t_n), x_2(t_n), \ldots, x_m(t_n)\right) \tag{3}$$

maps a Poincare section or "slice" of the chaotic attractor taken when one state variable is equal to a constant. A periodic orbit occurs when the series begins to repeat itself. The period ith orbit is defined by,

$$\xi_n = \xi_{n+i} \tag{4}$$

DETERMINE THE LOCAL DYNAMICS OF THE ORBIT

For simplicity we will examine the dynamics around a period one orbit, but the analysis also applies to higher orbits. Let $\xi_f \equiv 0$ be the fixed point along the periodic orbit. By changing the control parameter, p , the fixed point coordinates will translate to some other point close to the original fixed point, $\xi_f(\overline{p})$. Assuming that p=0 along the original orbit and that the changes in the system are small,

$$g \equiv \partial \xi_f(p) / \partial p\big|_{p=0} \cong \xi_f(\overline{p}) / \overline{p} \tag{5}$$

Using this approximation, the translation can then be linearized about the original orbit,

$$\{\xi_{n+1} - \xi_F(p)\} \cong [M] \cdot \{\xi - \xi_F(p)\} \tag{6}$$

where M is an m x m matrix. The dynamics around the point are found by substituting Equation 5 into Equation 6 and noting that the M matrix contains the direction vectors of the unstable and stable manifolds,

$$\{\xi_{n+1}\} \cong \{p_n g\} + [\lambda_u e_u f_u + \lambda_s e_s f_s] \cdot \{\xi_n - p_n g\} \tag{7}$$

where λ_u and λ_s are the unstable and stable eigenvalues, e_u and e_s are the unstable and stable unit eigenvectors, and f_u and f_s are contravariant basis vectors defined by

$$f_u \cdot e_u = f_s \cdot e_s = 1 \tag{8}$$

and

$$f_u \cdot e_s = f_s \cdot e_u = 0 \tag{9}$$

CONTROLLING THE SYSTEM

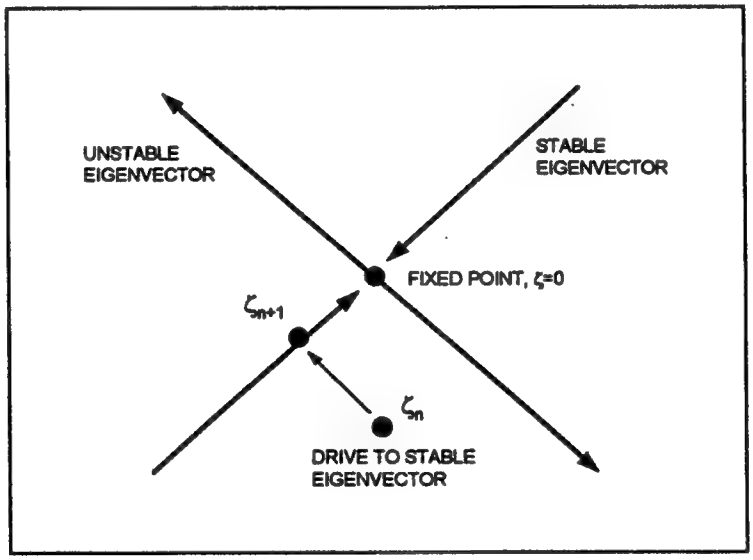

Figure 8. Chaotic Control of the *n*th Iteration

To stabilize the system, we drive the orbit, ξ_n, towards the stable manifold on the desired fixed orbit, $\xi_F \equiv 0$, as illustrated in Figure 8. This is accomplished by manipulating the accessible control parameter, p, such that

$$f_u \cdot \xi_{n+1} = 0 \tag{10}$$

The control parameter required to accomplish this can be calculated by substituting Equation 10 into Equation 7,

$$p_n = \lambda_u(\lambda_u - 1)^{-1}(\xi_n \cdot f_u)/(g \cdot f_u) \tag{11}$$

As the trajectory approaches this stable manifold, the system will collapse towards the fixed point. Once on the manifold we set p=0.

The operational range of such an algorithm is limited by the ability to vary the control parameter. Only small changes in the control parameter are desired,

$$p_* > p > -p_* \tag{12}$$

where p_* is the control threshold. The threshold is made small enough that the system's overall dynamics are not altered by variations in the parameter -- we do not want to create new orbits with different dynamics. Consequently, control is only enabled when

$$|\xi_n - \xi_F| < p_* \left|(1-\lambda_u)^{-1} g \cdot f_u\right| \tag{13}$$

along the unstable manifold. Outside of this range we will essentially turn the control off, recognizing that the system's chaotic nature will eventually drive it back into the controllable limits.

HENON ATTRACTOR MODEL

The Henon attractor control provides an excellent example of chaotic control methods. Let x and y be coordinates of a two dimensional Poincare section where,

$$x_{n+1} = A - x_n^2 + By_n \tag{14a}$$
$$y_{n+1} = x_n \tag{14b}$$

and A is the control parameter and B is held constant. Figure 9 illustrates the chaotic nature of the Henon attractor. We set a nominal value, A_o, for the control parameter and vary it by quantity by p,

$$A = A_0 + p \tag{15}$$

Our goal is to control the system about a period one orbit within the attractor so that,

$$\zeta_1 = \xi_2 = \xi_3 = \xi_n \tag{16}$$

Setting A_o=1.4 and B=0.3, the period one orbit results in a fixed point located at,

$$\xi_F = (x_F, y_F) \cong (0.884, 0.884) \tag{17}$$

The local dynamics around this point are linearized using Equation 6,

$$\begin{Bmatrix} x_{n+1} \\ y_{n+1} \end{Bmatrix} = [M]_1 \begin{Bmatrix} x_n \\ y_n \end{Bmatrix} \tag{18}$$

where M is a 2 x 2 direction matrix. In this case, the directional matrix is calculated analytically,

$$[M]_1 = \begin{bmatrix} \partial x_{n+1} / \partial x_n & \partial x_{n+1} / \partial y_n \\ \partial y_{n+1} / \partial x_n & \partial y_{n+1} / \partial y_n \end{bmatrix}_{\xi_1 = \xi_f} = \begin{bmatrix} -2 \cdot x_1 & 0.3 \\ 1 & 0 \end{bmatrix}_{\xi_1 = \xi_f} \tag{19}$$

Substituting Equation 17 into Equation 19, the corresponding unstable and stable eigenvalues and vectors around the fixed point are shown in Table 2 along with the eigenvalues and vectors of a period two and period four orbit. We used the same analysis to determine the local dynamics around those orbits where,

$$\begin{Bmatrix} x_{n+2} \\ y_{n+2} \end{Bmatrix} = [M]_2 [M]_1 \begin{Bmatrix} x_n \\ y_n \end{Bmatrix} \tag{20}$$

for period two orbits, and

$$\begin{Bmatrix} x_{n+4} \\ y_{n+4} \end{Bmatrix} = [M]_4 [M]_3 [M]_2 [M]_1 \begin{Bmatrix} x_n \\ y_n \end{Bmatrix} \tag{21}$$

for period four orbits.

ORBIT NO.	FIXED POINTS	UNSTABLE		STABLE	
		EIGEN VECTORS	EIGEN VALUES	EIGEN VECTORS	EIGEN VALUES
1	(0.884,0.884)	(-0.887,0.461)	-1.924	(0.163,1.043)	0.156
2	(-0.666,1.366)	(-0.928,0.373)	-3.009	(0.297,-1.197)	-0.030
4	(0.894,-0.989)	(0.884,0.467)	-8.637	(0.165,1.218)	-0.001

Table 2. Unstable and Stable Eigenvalues and Vectors for the Henon Attractor

Governed by Equation 11, the size of the controllable range for the period one orbit,

$$|\xi_n - \xi_F| < 0.1084 \tag{22}$$

Applying Equation 11 every time the state-space trajectory pierces this boundary forces the dynamical behavior of the system to eventually collapse onto the fixed point. Figure 10 shows the effects of our control on the Henon attractor.

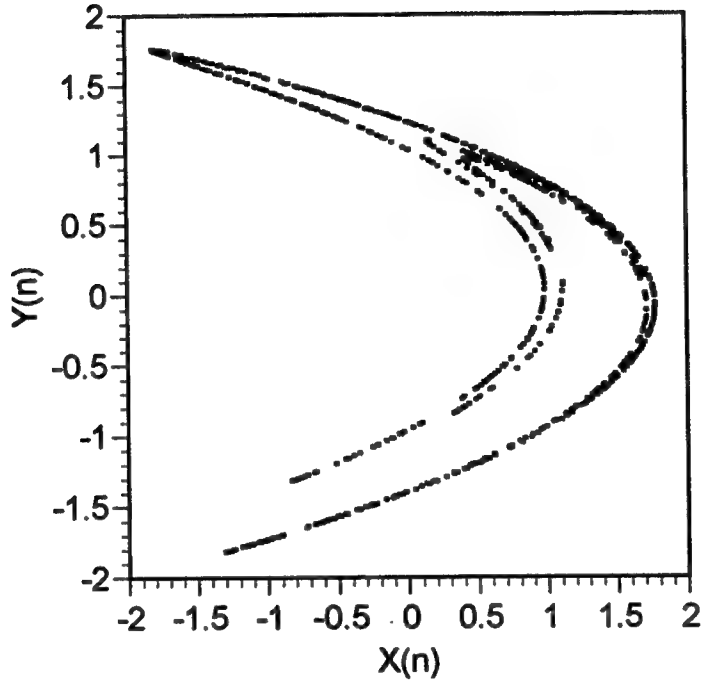

Figure 9. Poincare Section of the Henon Attractor

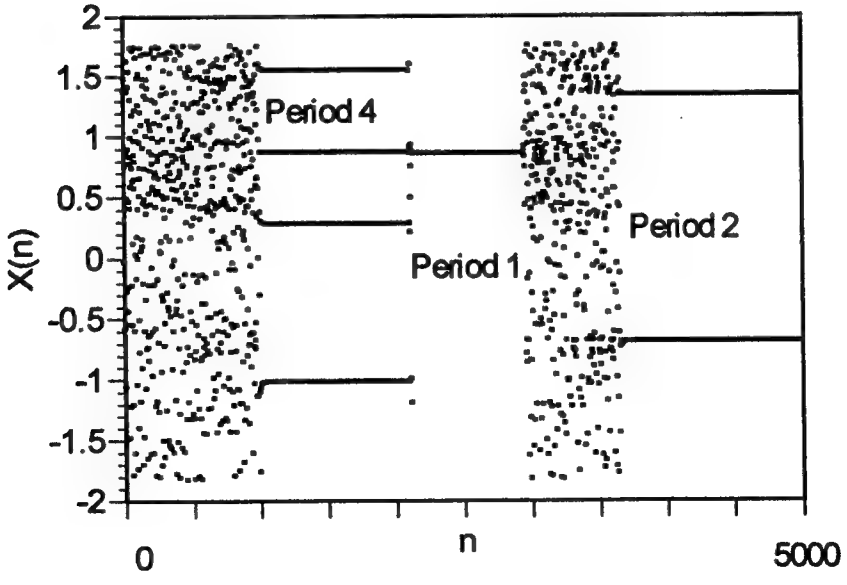

Figure 10. Chaotic Control of Henon Attractor

ER-MAGNETOELASTIC ATTRACTOR MODEL

The main objective for Phase I research is to simulate a computer model of a real physical structure incorporating ER materials. We want to evaluate the feasibility of introducing chaotic control algorithms into such structures for an experimental demonstration/validation prototype. We chose to model the magnetoelastic attractor.

Moon and Holmes[17] first investigated the magnetoelastic attractor. They modeled the behavior of a structure using a cantilevered Bernoulli-Euler beam vibrating in a magnetic field. Their model takes into account the kinetic energy of the beam, potential energy of the beam, potential energy of the magnetic field, and external work. For our project, we have modified their equations to account for ER material adaptability and an external electromagnetic forcing function.

ER material adaptability manifests itself in the flexural rigidity of the structural system. We modeled this parameter based on a composite structure with ER material sandwiched between two elastic constraining layers. Don et al.[18-20] investigated the theoretical dynamic behavior of such structures using the Ross, Kerwin, and Ungar[21] constrained layer damping models. The model accounts for ER material properties by assuming shearing motion within the sandwiched layer and incorporating these properties into an effective flexural rigidity. Equation 23 is the effective flexural rigidity,

$$\overline{EI} = E_1 I_1 + E_2 I_2 + E_3 I_3 + E_1 H_1 H_{10}^2 + E_2 H_2 H_{20}^2 + E_3 H_3 H_{30}^2 - \frac{E_2 I_2}{H_2}\frac{H_{31} - D}{1+g} - \left[\frac{E_2 H_2}{2} H_{20} + E_3 H_3 H_{30}\right]\frac{H_{31} - D}{1+g} \tag{23}$$

where

$$D = \frac{E_2 H_2 (H_{21} - H_{31}/2) + g(E_2 H_2 H_{21} + E_3 H_3 H_{31})}{E_1 H_1 + E_2 H_2 / 2 + g(E_1 H_1 + E_2 H_2 + E_3 H_3)} \tag{24}$$

and

$$g = \frac{G_2}{E_3 H_3 H_2 \lambda^2} \tag{25}$$

$E_i I_i$ is the flexural rigidity of the ith layer, λ is the wave number, and H_{i0} is the distance from the mid plane of the ith layer to a new neutral plane created by the addition layers two and three. The old neutral plane, defined as the neutral plane without any additional layers, is the mid plane of the first layer. Therefore,

$$H_{i0} = H_{i1} - D \tag{26}$$

where H_{i1} is the distance between the mid-plane of the ith layer and the mid-plane of layer one, and D is the displacement of the old neutral plane. Equation 25 incorporates shear behavior of the sandwiched layer where the value is a function of both the ER material and a sealant used to hold the fluid,

$$G_2 \cong \frac{A_{sealant}}{A_{total}} \cdot G_{sealant} + \frac{A_{ER}}{A_{total}} \cdot G_{ER} \tag{27}$$

where A represents the surface area of the respective material. The shear modulus of the ER material is found experimentally to be a function of the electric field squared,

$$G_{ER} = K \cdot V^2 \tag{28}$$

where K is an experimentally determined material constant and V is the applied electric field.

CONSTANT	DESCRIPTION	VALUE
K	ER Material Property Constant	15.34 kPa/kV/mm
E_{ER}	Elastic Modulus of ER material	0 Pa
E	Elastic modulus of layers 1 and 3	2.34 GPa
$G_{sealant}$	Shear modulus of the sealant material	0.5 MPa
H_1	Height of the 1st layer	7.94×10^{-4} m
H_2	Height of the 2nd layer	7.94×10^{-4} m
H_3	Height of the 3rd layer	7.94×10^{-4} m
λ	Wavenumber	10.29
w	Width of the structure	0.025 m
L	Length of the structure	0.305 m
η	Structural damping per unit length	.038 kg/s/m
β	Magnetic field constant	0.5 kg/m³/s²
α	Magnetic field constant	18.32 kg/m/s²
A_o	External Force Amplitude	0.28 N
Ω	Forcing frequency	0.89 rad/s
m	Mass per unit length	0.115 kg/m

Table 3. Physical Constants for the ER-Magnetoelastic Model

We substituted this effective flexural rigidity into a modified Moon and Holmes magnetoelastic system. The Moon and Holmes model assumed a moving reference frame as the external forcing function. For this investigation, a discrete forcing function actuates the structure at a point source. The resulting equation of motion for the system is,

$$m(x)\ddot{w} + \eta\dot{w} - \alpha w + \beta w^3 + \overline{EI}w = A_0 \sin(\Omega t) \tag{29}$$

where $m(x)$ is the mass per unit length, w is the horizontal position, η is the overall structural damping, A_o is the magnitude of the forcing function, and α and β are magnetic

field constants. This model assumes only first mode vibrational behavior and magnetic field affects only at the beam's tip. The state equations representing the dynamical equation of motion in Equation 29 are,

$$\begin{aligned} \dot{w}_0 &= \left(-\eta w_0 + \alpha w_1 - \beta w_1^3 - \overline{EI} w_1 + w_2\right) / m(x) \\ \dot{w}_1 &= w_0 \\ \dot{w}_2 &= A_0 \Omega \cos(\Omega t) \end{aligned} \qquad (30a,b,c)$$

where w_0 is the velocity of the beam, w_1 is the position of the beam, and w_2 the external forcing function. The physical modeling constants are defined in Table 3.

A three dimensional attractor shown in Figure 11 is found by iterating Equation 31,

$$W(t+\Delta t) = f(W(t)) \cdot \Delta t + W(t) \qquad (31)$$

where W is the set of state variables. Figure 12 shows a surface section or Poincare section of this three dimensional attractor taken at

$$t_n = \frac{2\pi n}{\Omega} \qquad (32)$$

A period three orbit is observed from this mapping such that,

$$\xi_n = \xi_{n+3} \qquad (33)$$

We selected to control the system using the fixed point located at,

$$\xi_F = (x_F, y_F) \cong (-0.404, -0.073) \qquad (34)$$

The corresponding eigenvalues and vectors are found by evaluating the behavior of several points around the fixed point. Table 4 describes the local dynamics.

UNSTABLE		STABLE	
EIGENVECTORS	EIGENVALUES	EIGENVECTORS	EIGENVALUES
(0.284,0.959)	23.00	(-0.595,0.804)	0.13

Table 4. Unstable and Stable Eigenvalues and Vectors for the Magnetoelastic Attractor

Figure 13 and 14 show the effects of our control algorithm on the state-space and time domains respectively.

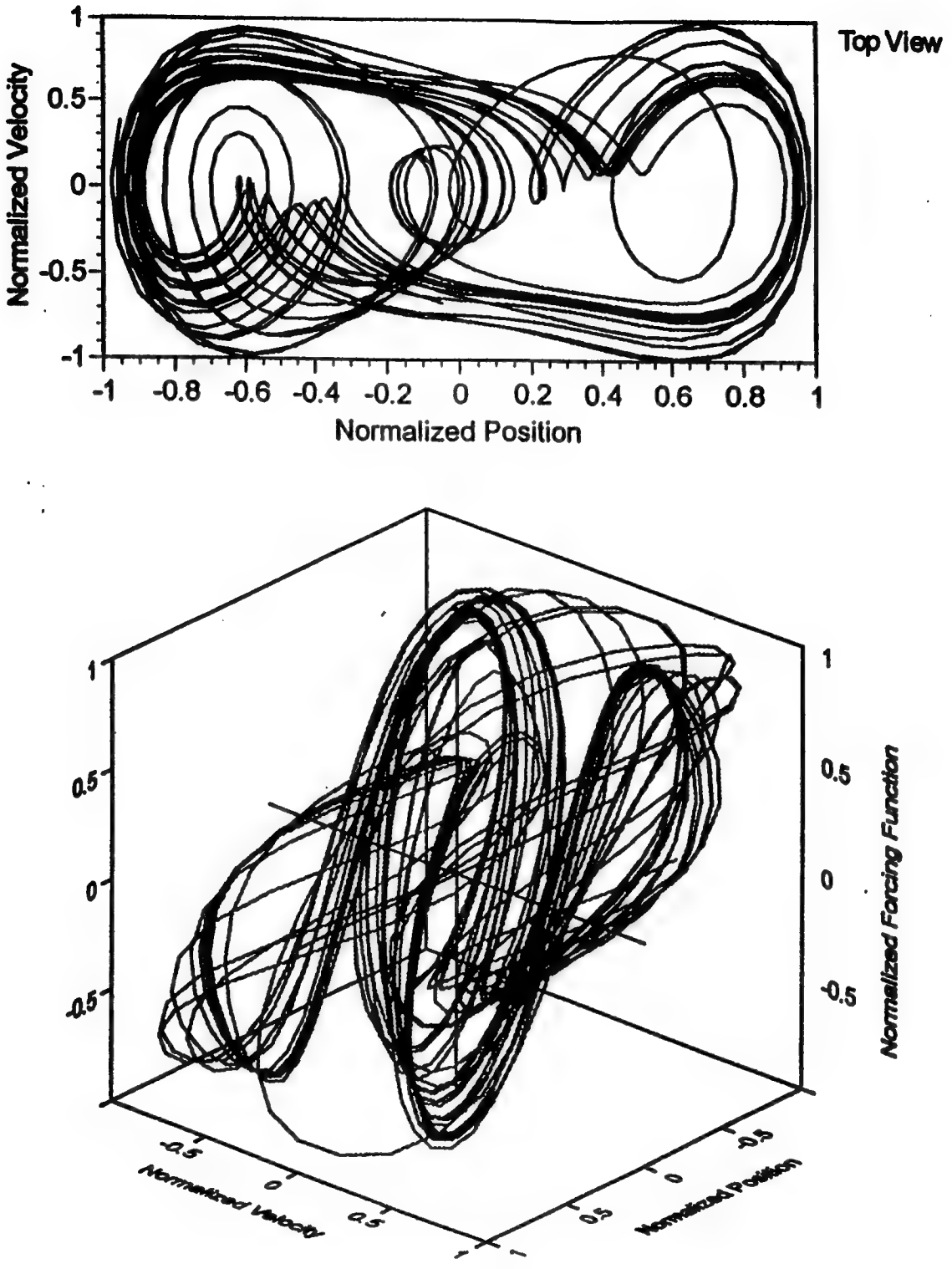

Figure 11. Computer Simulated Chaotic Behavior of a Magnetoelastic Attractor

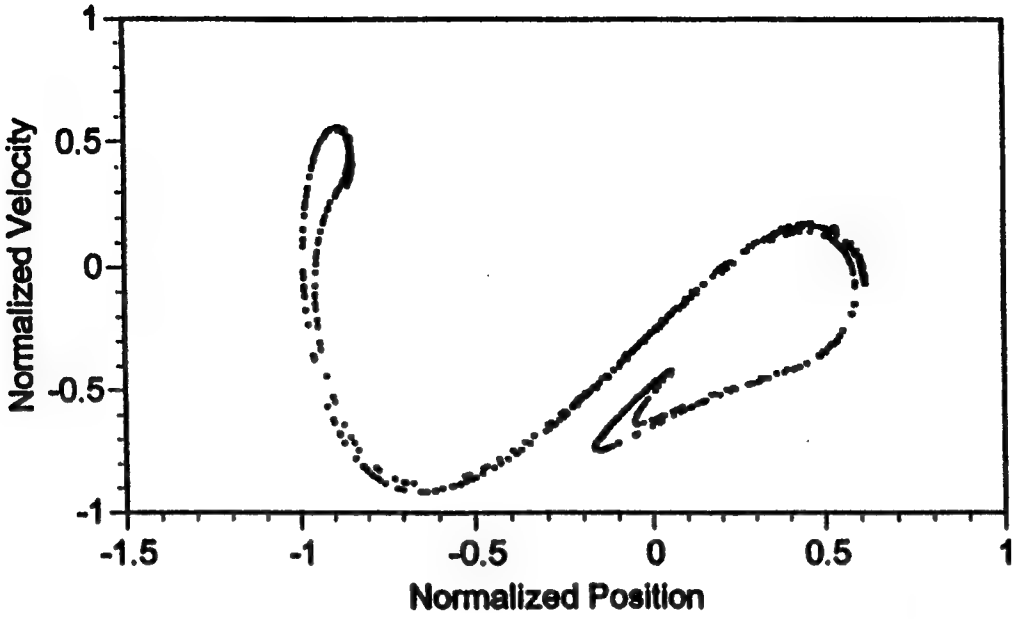

Figure 12. Computer Simulated Poincare Section of the Magnetoelastic Attractor

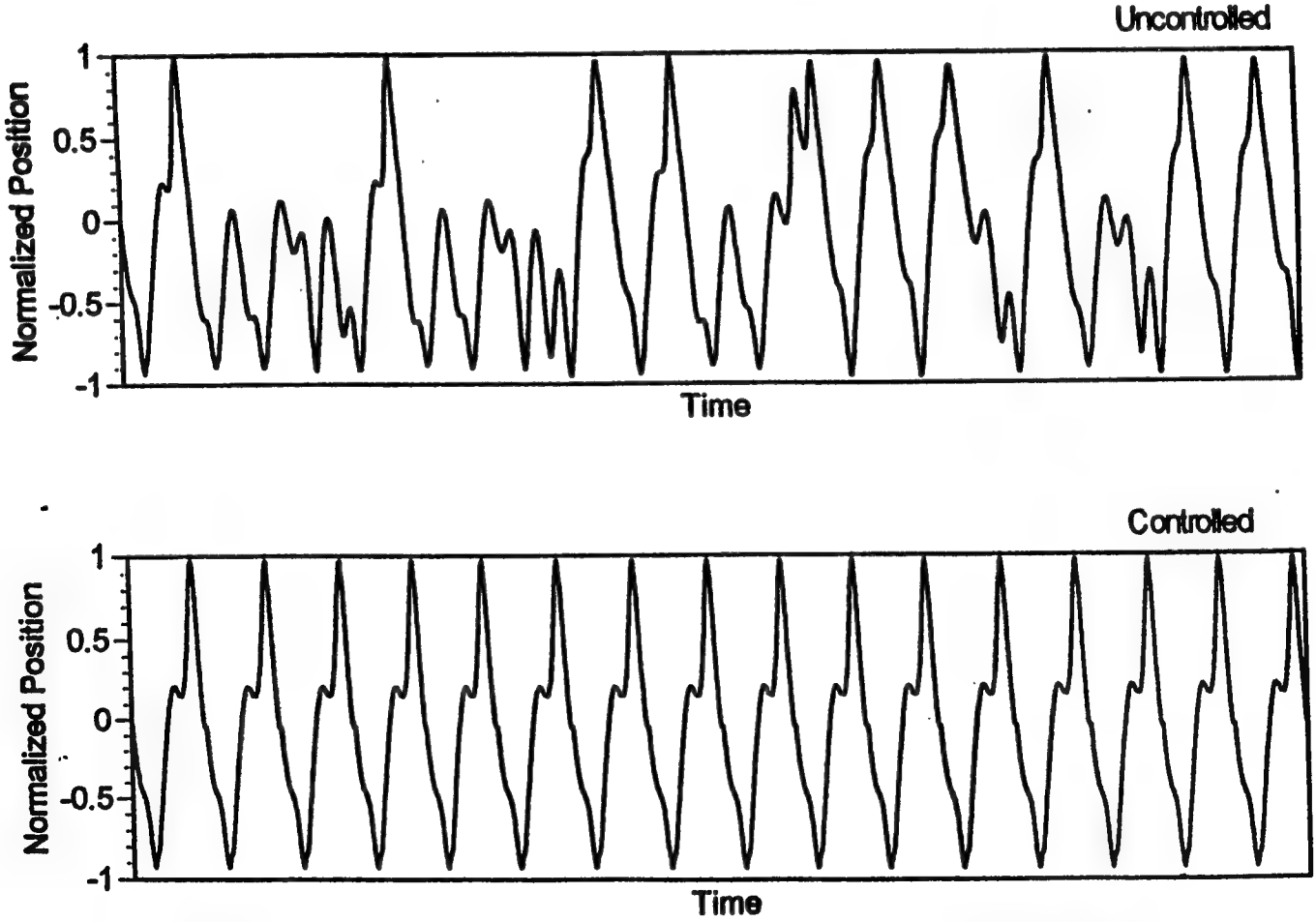

Figure 13. Computer Simulated Chaotic Control of the Magnetoelastic Attractor (Time)

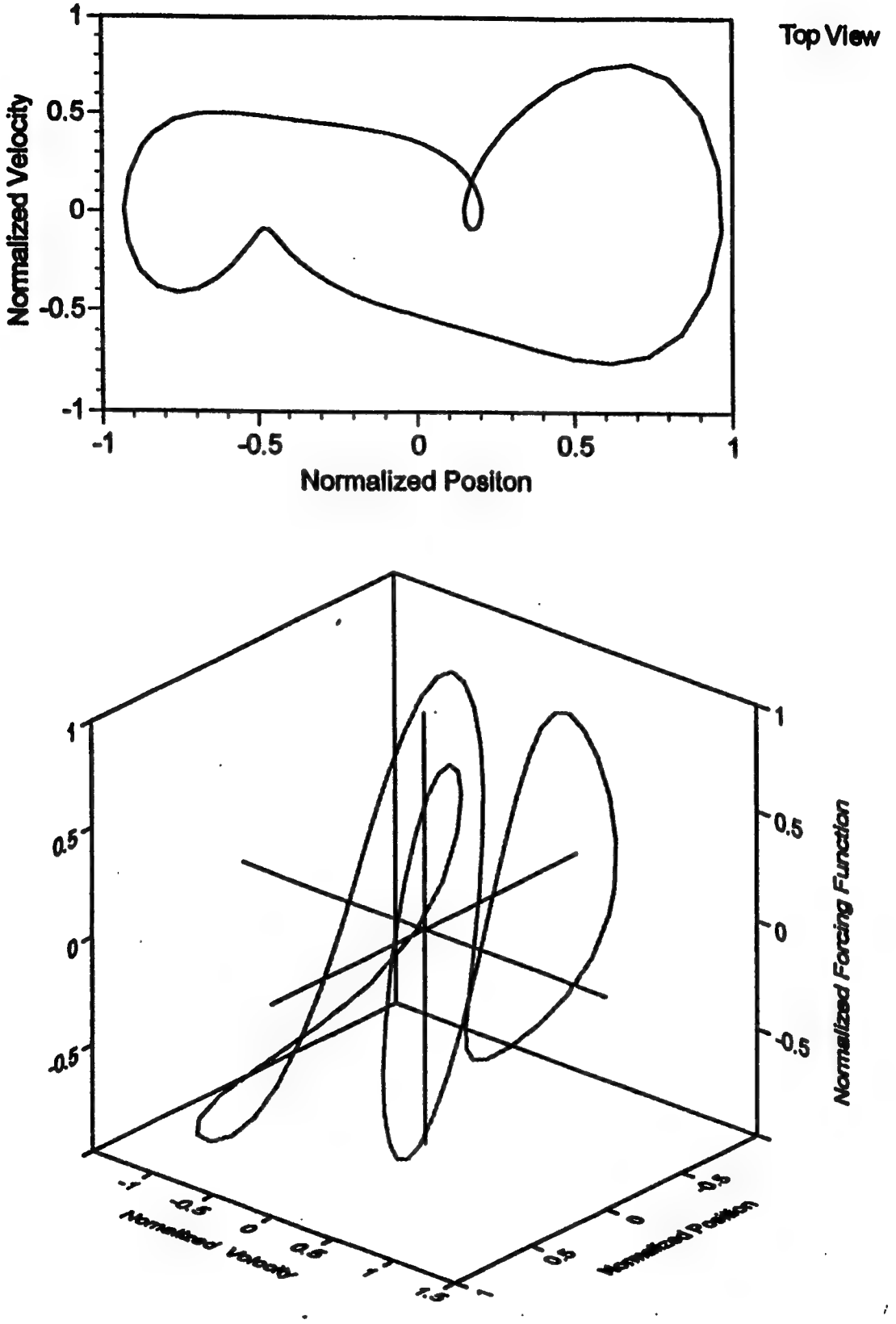

Figure 14. Computer Simulated Chaotic Control of the Magnetoelastic Attractor (State-Space)

EXPERIMENTAL MODEL

Our feasibility analysis includes a comparison between this computer simulation and an experimental model. We fabricated an electrorheological material adaptive structure composed of Lord Corporation Material, ER III, sandwiched between two polycarbonate sheets. Neoprene rubber adhered to the edges of the polycarbonate sealed the structure and acted as a spacer between the constraining layers. The adhesive was a 3M 847 Rubber and Gasket adhesive. A graphite coating, Grapho 206, applied to the surfaces of the polycarbonate sheets served as the electrodes. Figure 15 shows a schematic illustration of the structure and its dimensions.

A detailed illustration of the experimental testbed is shown in Figure 16. A Bently Nevada 3040 HTB electromagnetic probe actuated the structure while an AROMAT 30mm Laser Proximity Sensor measured the vibrational amplitude. Two rectangular magnets attached on a platform at the end of the beam produced the magnetic field. All relevant data was recorded using a PC based acquisition system supplied by National Instruments.

The Figures 17 and 18 illustrate the chaotic behavior and Poincare Section respectively, while Figure 19 shows the orbits we desire to stabilize.

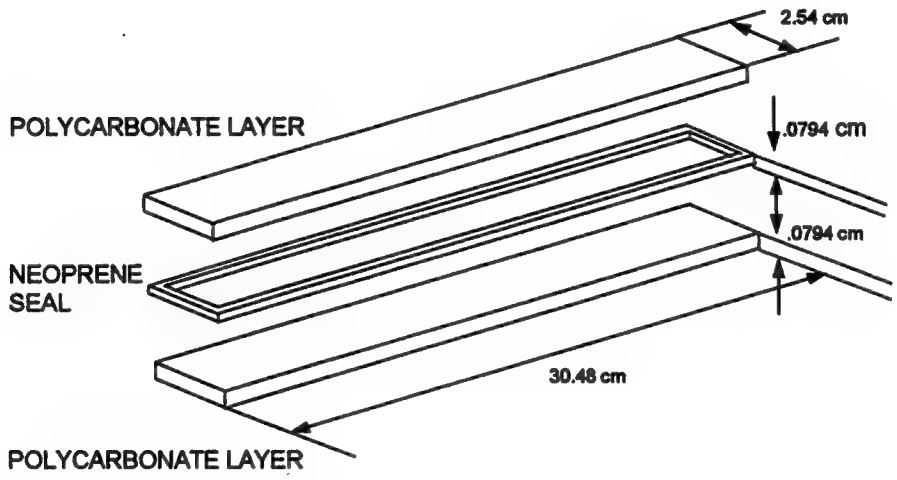

Figure 15. Experimental ER Material Composite Structure

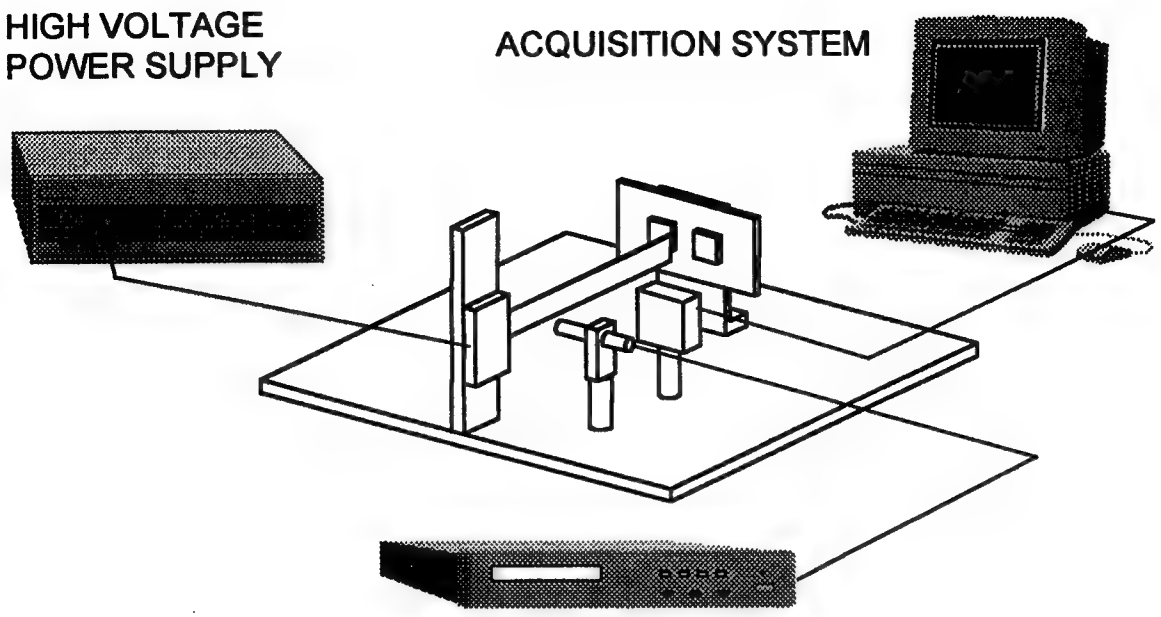

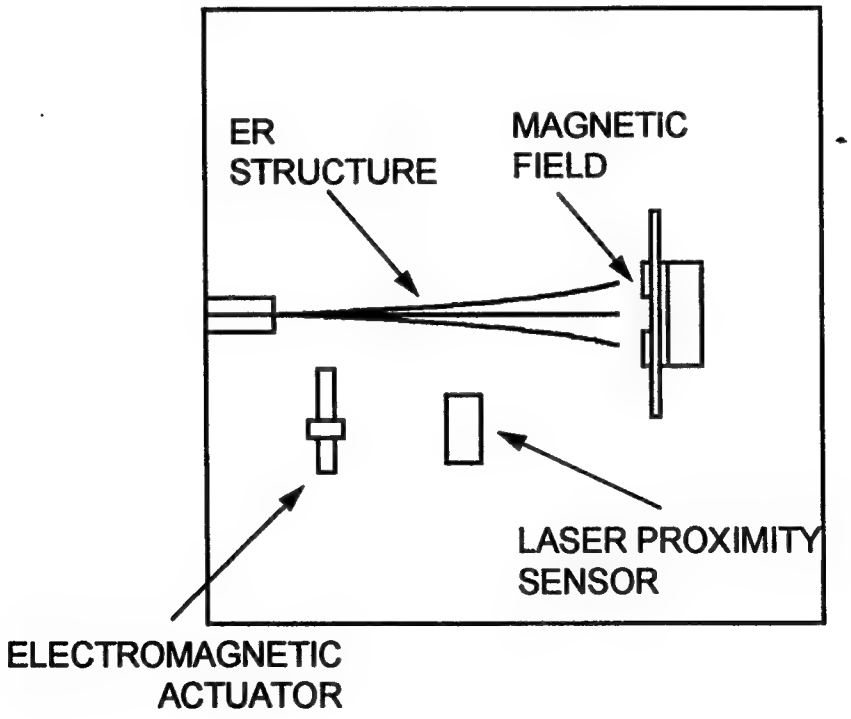

Figure 16. Schematic of the Experimental Testbed

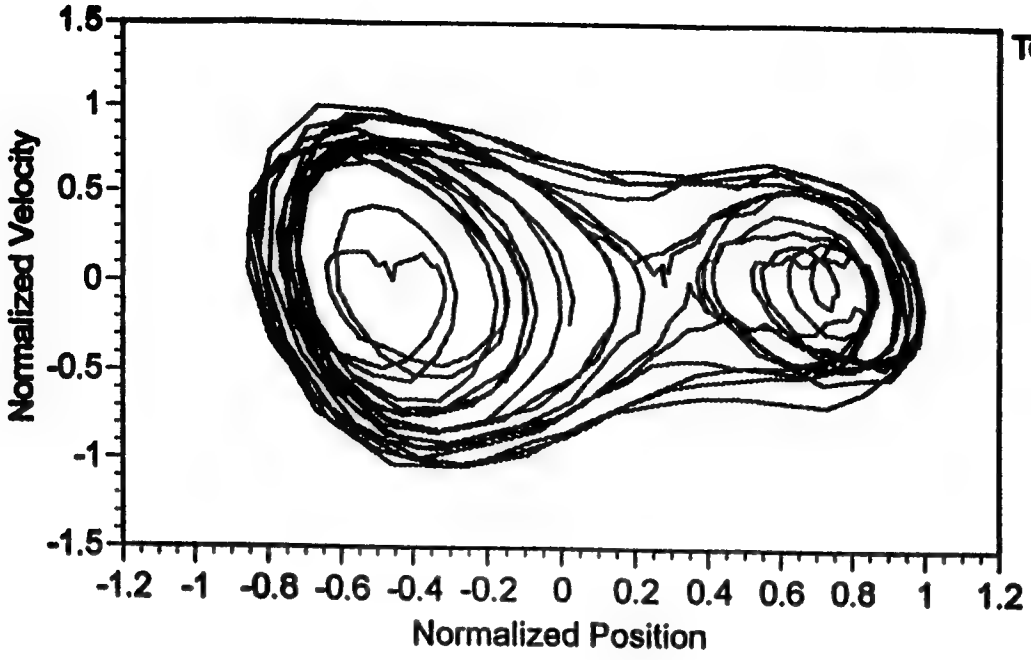

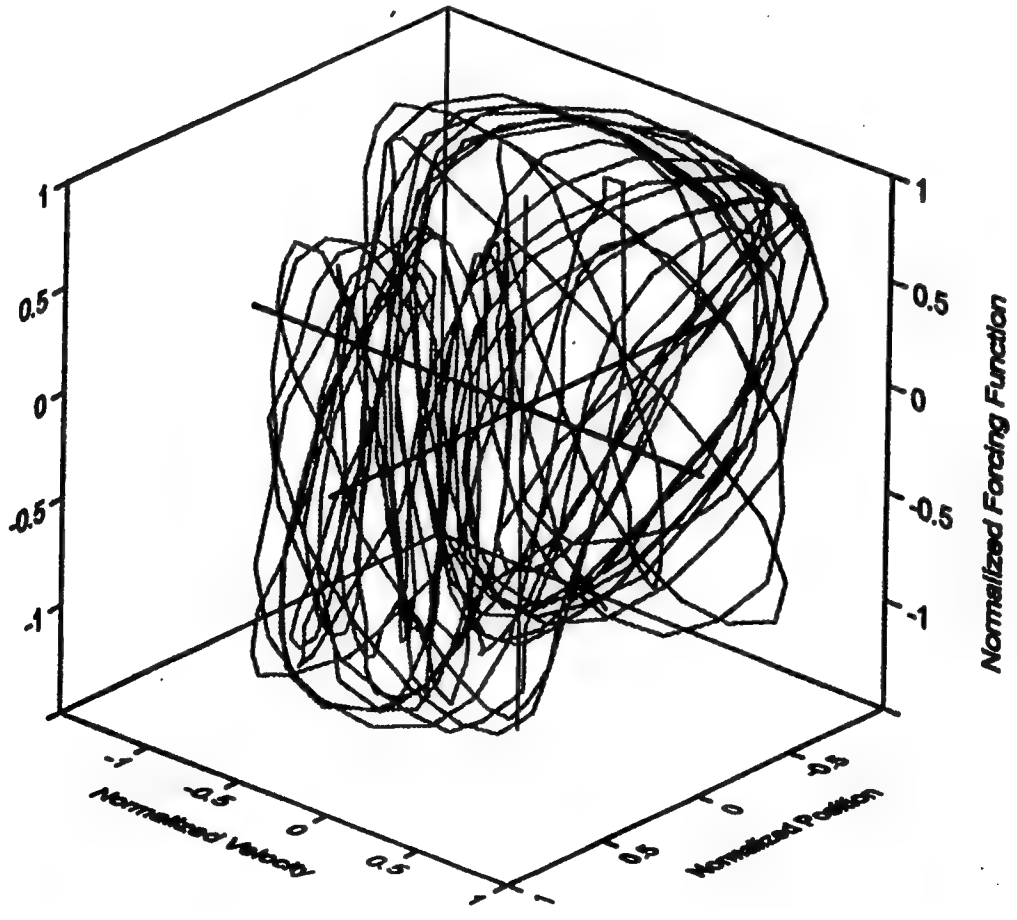

Figure 17. Experimental Chaotic Behavior of a Magnetoelastic Attractor

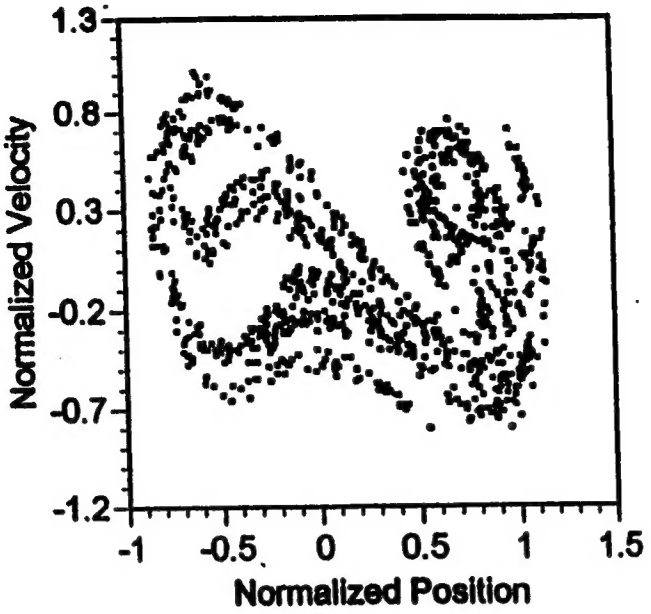

Figure 18. Experimental Poincare Section of the Magnetoelastic Attractor

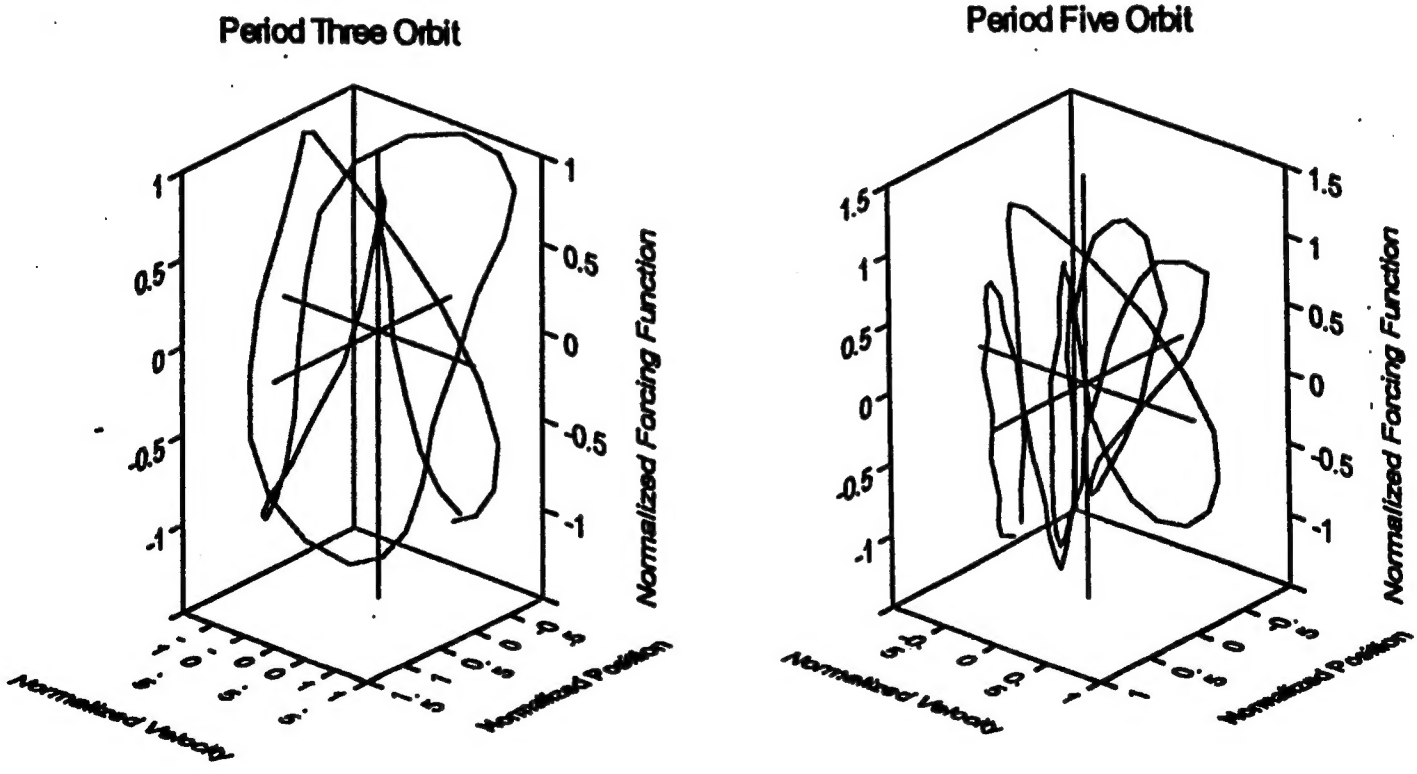

Figure 19. Experimental Period 3 and Period 5 Orbits

IV. SUMMARY OF IMPORTANT RESULTS

- Periods one, two, and four orbits within a Henon attractor were effectively stabilized.
- The chaotic algorithm applied to the ER-magnetoelastic computer model effectively stabilized the system about a period three orbit.
- The computer model of the ER-magnetoelastic system agreed qualitatively with the experimental simulation.
- We observed period three and period five orbits within the experimental ER-magnetoelastic attractor

V. DISCUSSION

The most important result from our research is that chaotic controls can be implemented onto a computer simulated model and that the simulation qualitatively resembles a real physical structure. Chaos is a "visual" science where qualitative behavior is more important than quantitative equivalence. Exact "scale" between theory and experiment is trivial. These simulations are used as tools to quantify qualitative behavior where we ask -- What degree of chaos and types of attractors can we control?

Though there are visual differences in the attractor models, the forms of the attractor are qualitatively similar. A comparison of the theoretical and experimental attractors shown in Figures 11 and 17 illustrate this similarity. The noticeable differences most likely result from the experimental structure's deviations from pure sinusoidal mode shapes and the reliability of the rheological property data. The theoretical model uses an approximation of an effective flexural rigidity of a 3 layer composite structure. The flexural rigidity is based on the Ross, Kerwin, and Ungar (RKU) [21] damping model that only assumes pure sinusoidal mode shapes. A cantilevered beam does not have pure sinusoidal mode shapes especially at lower frequencies. In this investigation, we are actuating a cantilevered structure at frequencies where mode 1 behavior dominates. We believe some of the differences in theoretical and experimental results arise from this RKU assumption. In addition, Yalcintas et al. [20] have questioned the reliability of the rheological behavior data obtained on these ER materials. More rheology testing is clearly needed.

Since we are able to control the computer model of the ER-magnetoelastic system and the experimental model qualitatively agrees with the computer simulation, we believe that those same chaotic algorithms can control the physical experiment. Figures 14 and 19 show the theoretical and experimental orbits we desire to control.

VI. CONCLUSION

We believe we can stabilize the chaotic attractor of the ER magnetoelastic system.

VII. FURTHER RESEARCH AND DEVELOPMENT

There are several issues that need to be addressed before we can bring products like this into the marketplace. The following section defines our objectives and the questions we need to answer before a commercial product could become available.

1. Simulate Chaotic Vibration Control

- What types of chaotic attractors can we control?
- What are the best algorithms to use?
- What are the limitations of chaotic control?

2. Fabricate Prototype Chaotic Motion Stabilizers

- What degrees of chaos can we control?
- What are the physical limitations?
- How robust is the controller?
- How will these systems be manufactured?

3. Integrate Stabilizer with Controls for Real World Applications

- Are chaotic vibrations effective in real world environments?

4. Investigate the Rheological Behavior of ER Materials

- What are the best fluids to use for each application?
- How reliable is the long term fluid behavior?
- What are the effects of temperature on fluid behavior and reliability?

5. Investigate other Methods to Change the System Parameters

- What other controllable materials could we use to implement a Chaotic Motion Stabilizer?

VIII. REFERENCES

1. Block, H. and J.P. Kelly, *Electro-rheology.* J. Phys. D: Appl. Phys., 1988. 1: p. 1661-1677.
2. Gast, A.P. and C.F. Zukoski, *Electrorheological Fluids as Colloidal Suspensions.* Advances in Colloid and Interface Science, 1989. 30: p. 153-202.
3. Jordan, T.C. and M.T. Shaw, *Electrorheology.* IEEE Transactions on Electrical Insulation, 1989. 24(5): p. 849-878.
4. Weiss, K.D., J.P. Coulter, and J.D. Carlson. *Electrorheological Materials and Their Usage in Intelligent Material Systems and Structures, Part I: Mechanisms, Formulations and Properties.* in *Recent Advances in Adaptive and Sensory Materials and Their Applications.* 1992. Blacksburg, Virginia: Technomic Publishing Co., Inc.
5. Coulter, J.P., K.D. Weiss, and J.D. Carlson. *Electrorheological Materials and Their Usage in Intelligent Material Systems and Structures, Part II: Applications.* in *Recent Advances in Adaptive and Sensory Materials and Their Applications.* 1992. Blacksburg, Virginia: Technomic Publishing Co., Inc.
6. Ott, E., C. Gregobi, and J.A. Yorke, *Controlling Chaos.* Physical Review Letters. Physical Review Letters, 1993. 64(11): p. 1196.
7. Ott, Grebogi, C., Romeiras, F., and Yorke, J.A., Critical Exponents for Crisis-Induced Intermittancy, Physical Review letters, 1987, 36(11):p. 5365.
8. Hunt, E.R., High-Period Orbits Stabilized in the Diode Resonator, 1st Experimental Chaos Conference, Arlington, VA, 1991.
9. Shinbrot, T., Grebogi, C., Ott, E., Yorke, J.A., Using Small Perturbations to Control Chaos, Nature, 1993, 363(6428): p. 411-17.
10. Dressler, U. and Nitsche, G., Controlling Chaos Using Time Delay Coordinates, Physical Review Letters, 1991, 86(1): p.1.
11. Ditto, W.L., S.N. Rauseo, and M.L. Spano, *Mastering Chaos.* Scientific American. Scientific American, 1990. (August): p. 78.
12. Ditto, W.L., S.N. Rauseo, and M.L. Spano, *Experimental Control of Chaos.* Physical Review Letters. Physical Review Letters, 1990. 65(26): p. 3211.
13. Hall, E.K., and Hanagud, S.V., Control of Nonlinear Structural Dynamic Systems: Chaotic Vibrations, Journal of Guidance, Control, and Dynamics, 16(3): P. 470-6.
14. Rollins, R.W., Parmananda, P., and Sherard, P., Controlling Chaos in Highly Dissipative Systems: A Simple Recursive Algorithm, Physical Review E, 47(2): p. R780-3.
16. Garfinkel, A., Spano, M.L., Ditto, W.L., and Weiss, J.N., Controlling Cardiac Chaos, Science, 1992, 257: p 1230-35.
17. Moon, F.C., and Holmes, P.J., A Magnetoelastic Strange Attractor, Journal of Sound and Vibration, 1979, 65(2): p. 275-96.
18. Don, D.L., *An Investigation of ER Material Adaptive Structures.* 1993, Lehigh:
19. Don, D.L. and J.P. Coulter, *An Analytical and Experimental Investigation of ER Material Based Adaptive Beams.* Journal of Intelligent Materials and Systems. Journal of Intelligent Materials and Systems, Submitted 1993.
20. Yalcintas, M., J.P. Coulter, and D.L. Don, *Structural Modeling and Optimal Control of ER Material Based Plates.* ASME Journal of Vibration and Acoustics. ASME Journal of Vibration and Acoustics, Submitted 1993.
21. Ross, D., E.E. Ungar, and E.M. Kerwin, *Damping of Plate Flexural Vibrations by means of Viscoelastic Laminate.* Structural Damping. Structural Damping, 1959. ASME: p. 49-88.
22. Crutchfield, J.P., Farmer, J.D., Packard, N.H., Shaw, R.S., *Chaos,* Scientific American, 1986, 255: p46-57.